Supporting Information for

Thermodynamic and kinetic parameters for calcite nucleation on peptoid and model scaffolds- A step toward nacre mimicry

Anne R. Nielsen[a], Stanislav Jelavić[a,d], Daniel Murray[b,e], Behzad Rad[b], Martin P. Andersson[a,f], Marcel Ceccato[a,g], Andrew C. Mitchell[c], Susan L.S. Stipp[a,h], Ronald N. Zuckermann[b], Karina K. Sand[c,d]*

[a]Nano-Science Center, Department of Chemistry, University of Copenhagen, Denmark.

[b]Biological Nanostructures Facility, The Molecular Foundry, Lawrence Berkeley National Laboratory, Berkeley, California, USA.

[c]Department of Geography & Earth Sciences, Aberystwyth University, United Kingdom.

[d]Current address: GLOBE Institute, University of Copenhagen, Denmark.

[e]Current address: Idaho National Laboratory, Idaho Falls, ID, 83415, USA.

[f]Current address: Chemical Engineering, Technical University of Denmark, Denmark.

[g]Current address: iNano, Department of Chemistry, Aarhus University, Denmark.

[h]Current address: Physics, Technical University of Denmark, Denmark.

*Corresponding author: kks@sund.ku.dk

TABLE OF CONTENTS:

Characterization of SAM functionalized substrates:

X-ray photoelectron spectroscopy (XPS) of SAM functionalized substrates

We used XPS to study the elemental composition of the functionalized substrates. From small shifts in binding energy, we could gain insight into the chemical state of the elements. We used a Kratos Axis Ultra[DLD] spectrometer operating with Al monochromatic K_α radiation (1486.6 eV; 150 W). All data were collected at room temperature. The spectra were fit using the software CasaXPS. For fitting the background contribution, we used a Shirley or a linear function, as appropriate. The spectra were calibrated to the Au 4f peak at 84.2 eV that came from the substrate. The photoelectron peaks were fit using 30% Gaussian and 70% Lorentzian contributions.

Alkane thiol SAMs on Au substrates:

Figure S1 shows an XPS wide spectrum of the carboxyl SAM. We detected only elements from the Au-substrate and the $HS(CH_2)_{10}COOH$. The high resolution C 1s spectrum (Fig. S1, inset) contains contributions from the aliphatic carbon (C-C or C-H, 285.0 eV) and the carboxyl group (O=C-O(H), 289.5 eV). Small peaks between the two main peaks are ascribed to C-S and C-OH.
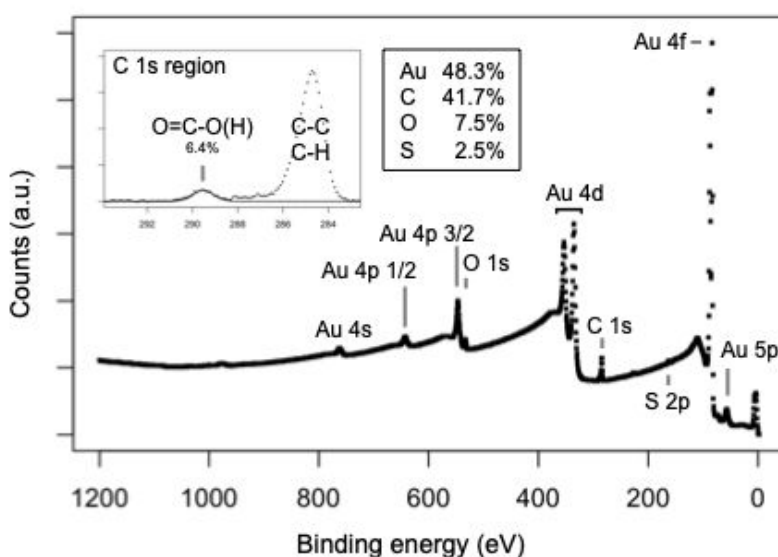

Figure S1: XPS wide scan of the carboxylic SAM functionalized surface prepared using acetic acid as a dispersion agent. Inset is the C 1s high resolution spectrum, which shows that the carboxyl group accounts for 6.4% of the total carbon.

Figure S2 shows the XPS wide spectrum for the amine SAM. We detected the elements from the Au-substrate and the

$HS(CH_2)_{11}NH_2$ with some Cl that was left from the rinsing procedure. The high resolution N 1s spectrum (Fig. S2, inset)

showed that the distribution between protonated and deprotonated amine was 1:2.
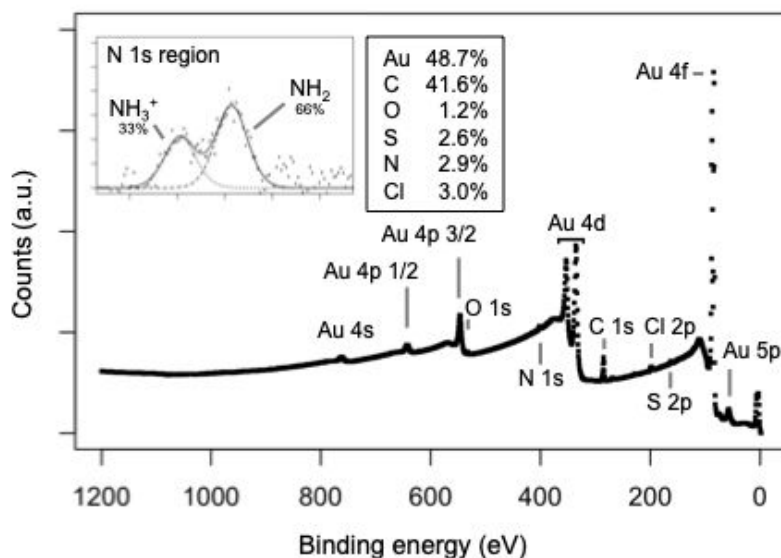

Figure S2: XPS wide scan of the amine SAM prepared using triethylamine as a dispersion agent. The inset in the figure is the N 1s high-resolution spectrum showing protonated and deprotonated amine.

Ratio of bound to unbound S in the alkane thiol SAMs:

To evaluate the success of thiol binding to Au substrates, we compared the amount of Au bonded sulfur to adsorbed

sulfur for each of the substrates. As an example, Figure S3 shows the S 2p high resolution spectrum for the carboxyl

functionalized substrate. There are two 2p doublets, one representing S bonded to Au and the other, physisorbed S.

For the carboxyl SAM, 73% of the thiol molecules were bound. For the amine SAM, 75% of the thiol molecules were

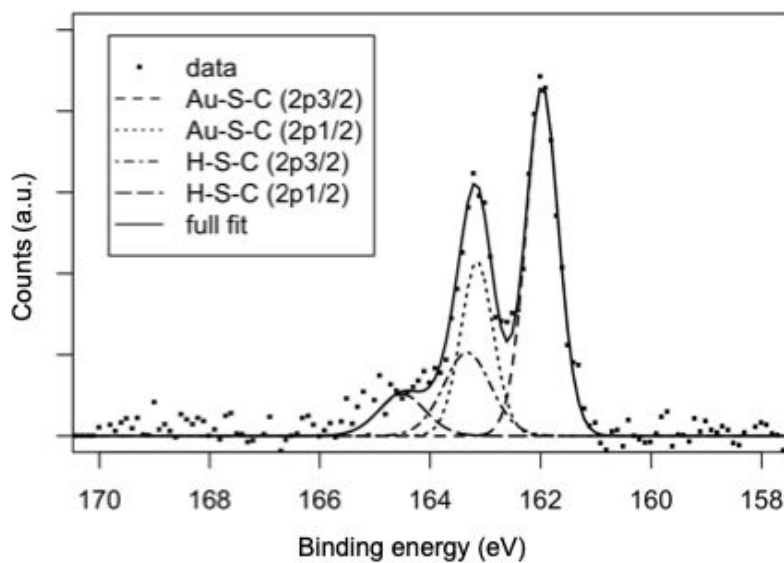bound and for the mixed SAM, ~76% were bound.

Figure S3: S 2p high resolution spectrum of the carboxyl SAM.

Quantification of COO(H) : NH₂ on mixed SAM:

We used the mixed SAMs as a model for B28 peptoid polymers. The B28 peptoid has the same amount of exposed carboxyl and amine functional groups, thus for our thiol model surfaces we aimed to prepare a 50/50% 11-mercapto-undecanoic acid to 11-amino-1-undecanethiol hydrochloride mixed SAM. The ratio of carboxyl and amine was estimated by quantifying the contribution of the carboxyl peak to the nitrogen peak from the high resolution spectra. We observed that the mixed SAM, prepared using 90 vol. % 11-mercapto-undecanoic acid and 10 vol. % 11-amino-1-undecanethiol hydrochloride resulted in a final coverage of ~50/50% (± 5%) of carboxyl to amine groups.

Investigation of CaCO$_3$-functionalized substrates:

Illustration of the nucleation rate setup:

Figure S4 shows a schematic drawing of the experimental setup used to measure nucleation rate. Upstream to the flow cell is a static mixer, which ensures mixing of the CaCl$_2$ and the NaHCO$_3$ solutions. Because the mixed solution is supersaturated, we used a mixer with a volume of only 50 µL and tubing with 0.5 mm inner diameter, to minimize the dead volume between the inlet of the static mixer to the sample.
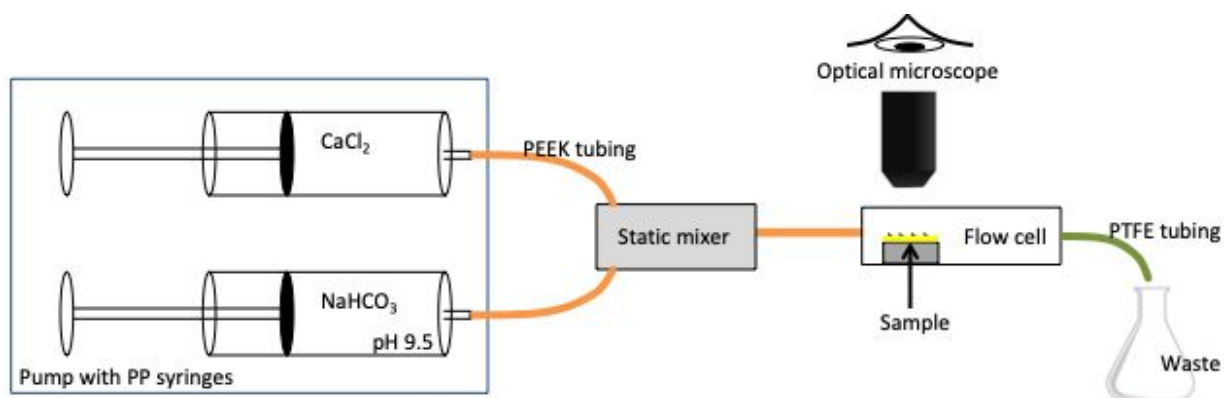

Figure S4: Schematic drawing of the nucleation rate setup. PP - polypropylene, PEEK - polyether ether ketone, PTFE - polytetrafluoroethylene.

Nucleation rate on functionalized substrates

Solution chemistry determined from PHREEQC calculations:

From PHREEQC,[1] we obtained the activity of the ions and saturation with respect to calcite.

Table S1: Solution composition determined using PHREEQC for the final mixed solutions.

Final concentration	Activity {Ca^{2+}} [10^{-3}]	Activity {CO$_3^{2-}$} [10^{-4}]	$\sigma_{calcite}$*
7 mM	3.182	1.977	5.25
8 mM	3.491	2.155	5.44
9 mM	3.784	2.328	5.57
10 mM	4.062	2.497	5.73
11 mM	4.328	2.662	5.85

*defined using *ln*, not *log$_{10}$*

Optical microscopy images obtained during nucleation rate studies:

Figures S5-S7 show example images obtained during the nucleation rate studies on carboxyl, amine and mixed SAMs, obtained at t = 10 s, 300 s and 850 s for each SAM at σ = 5.57. Because the sample surface is under the microscope with the functionalized side up, homogenous precipitation of particles can occur on the surface. Homogenously nucleated crystals are distinguished from the heterogeneously nucleated crystals by detection of particle movement. All crystals counted as heterogenously grown were thus first detected on the surface spot where they grew. For the substrates with a long incubation time and low nucleation rate, the solution is not deprived of ions at rates fast enough and becomes increasingly supersaturated. However, when ions from the solution are being consumed for heterogeneous nucleation, the homogenous nucleation rate decreases. The induction time at the carboxyl SAM was low and the nucleation rate relatively fast, thus homogeneous nucleation was not observed for any of the applied saturation levels. The resolution limitation of this method can result in some miscount, which leads to larger uncertainty on J_0 for surfaces with few nucleation sites.
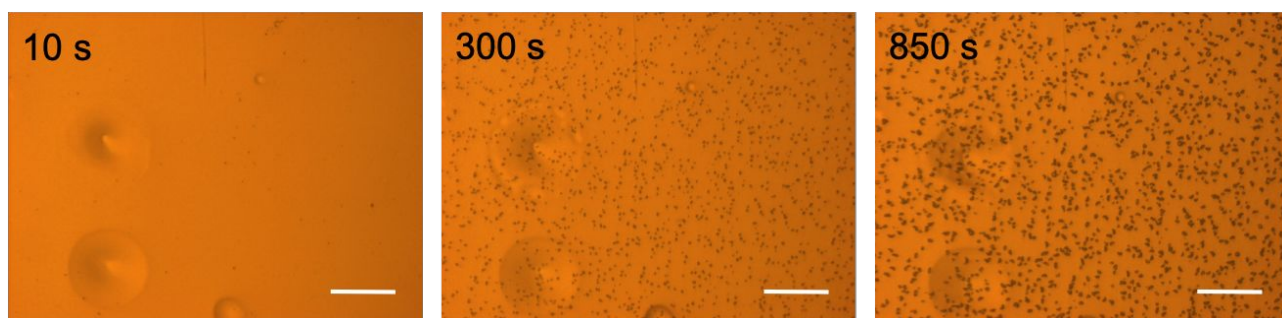

Figure S5: Optical microscopy images of carboxyl SAMs. All crystals nucleated heterogeneously. Scale bar is 100 μm.
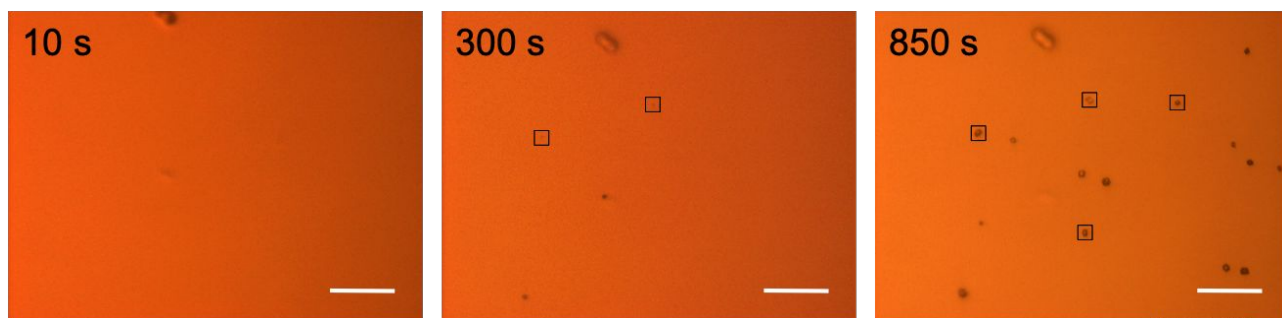

Figure S6: Optical microscopy images of amine SAMs. Crystal sites framed by squares have nucleated heterogeneously on the surface; others nucleated homogenously in solution (which we know because they move during the experiment, and landed on the substrates as large particles). These are ignored during the rate analysis. Scale bar is 100 μm.
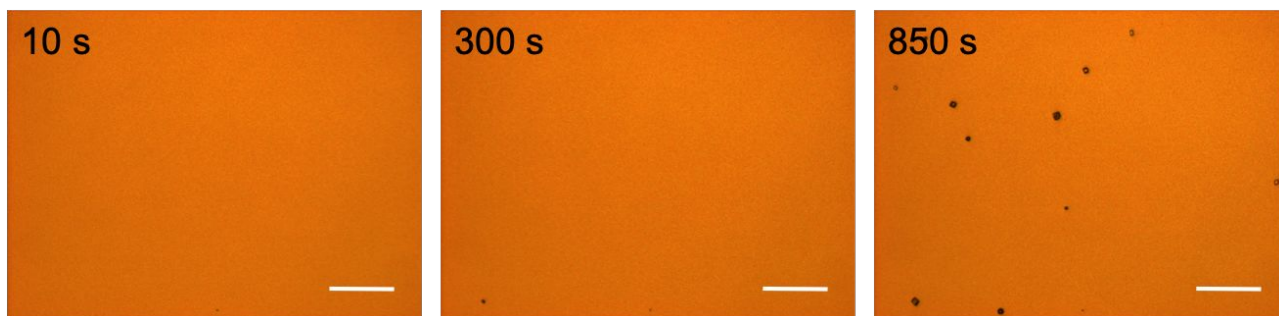
Figure S7: Optical microscopy images of mixed SAMs. All crystals nucleated homogenously in solution. We know this because they moved in the field of view during the experiment. Scale bar is 100 µm.

Figure S8 shows images obtained during the nucleation rate studies on B28 peptoid HOPG atr σ = 5.85. The step edges come from the topography of the underlying HOPG surface.
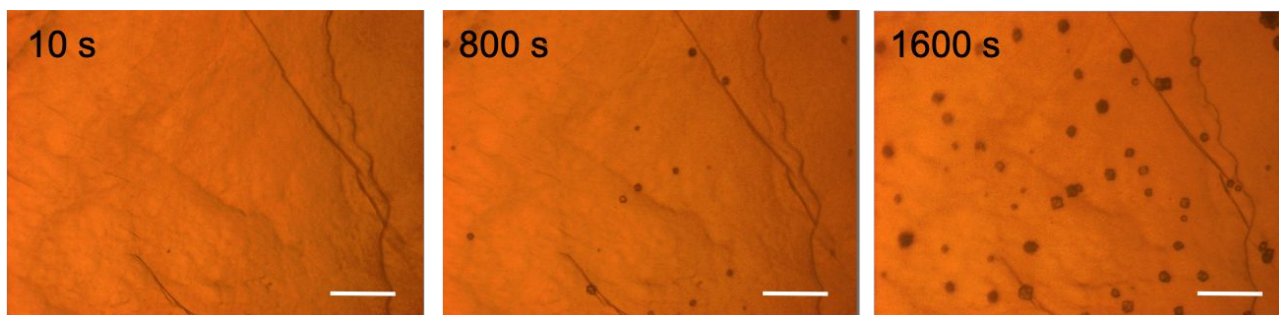

Figure S8: Optical microscopy images of B28 peptoids on HOPG surface after flow experiment. Scale bar is 100 µm.

Functionalized substrates after nucleation, imaged with SEM:

To deduce from which planes crystals nucleated, we used SEM to image the functionalized surfaces after the nucleation rate studies. Figure S9 and S10 show images at various magnifications for experiments carried out on the carboxyl and amine SAMs. Figure 11 shows the B28 peptoid on highly ordered pyrolitic graphite (HOPG), imaged after flow at σ = 5.85. As a reference study, we also imaged a freshly cleaved HOPG surface without the peptoid polymers, after flow experiments with σ = 5.85 (Fig. S12). On the freshly cleaved HOPG surface, the particle shape suggests vaterite, whereas crystals with calcite morphology grew on the B28 peptoid substrate.
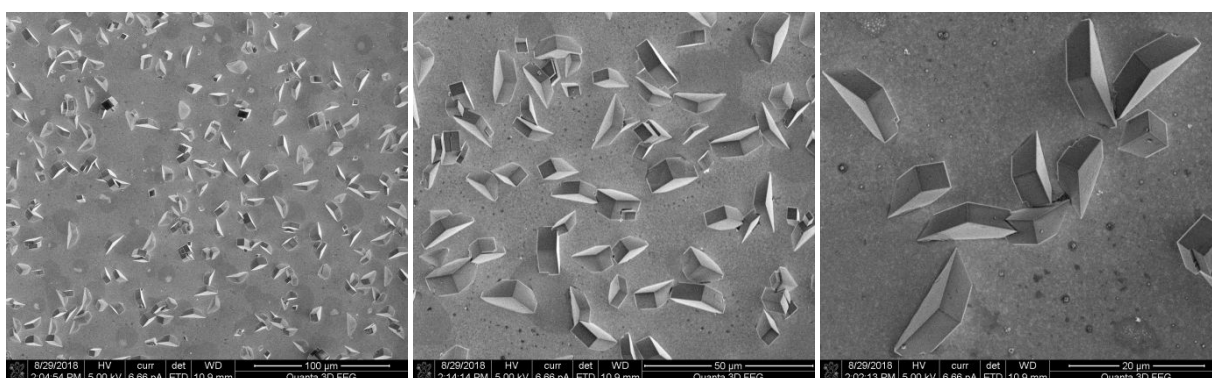

Figure S9: SEM photomicrographs of calcite crystals nucleated on the carboxyl SAM, obtained after the flow experiment at σ = 5.57.

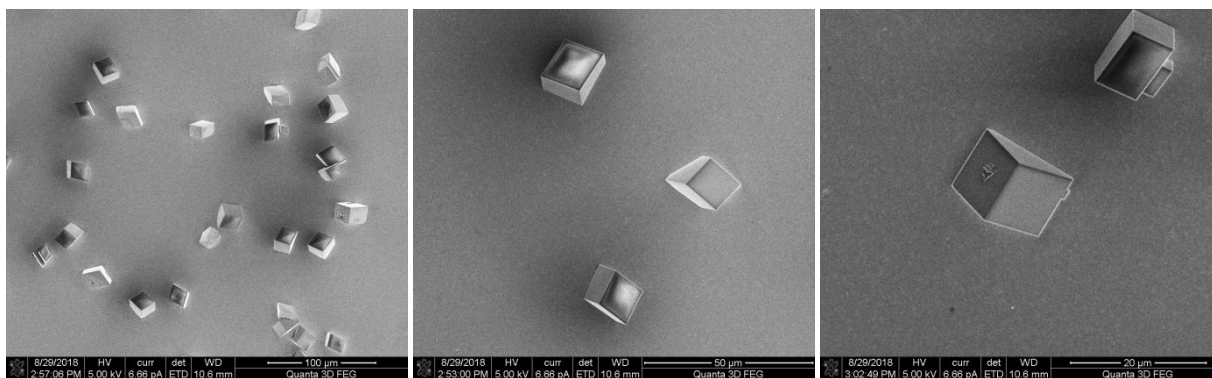Figure S10: SEM photomicrographs of the calcite crystals grown on the amine SAM obtained after the flow experiment at σ = 5.57.
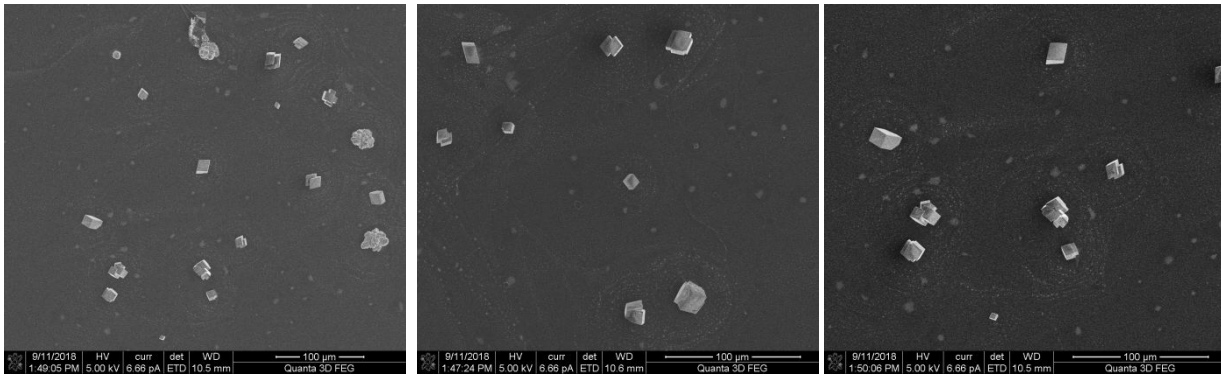
Figure S11: Calcite crystals grown on self-assembled B28 peptoid polymer substrates after the flow experiment at σ = 5.85.
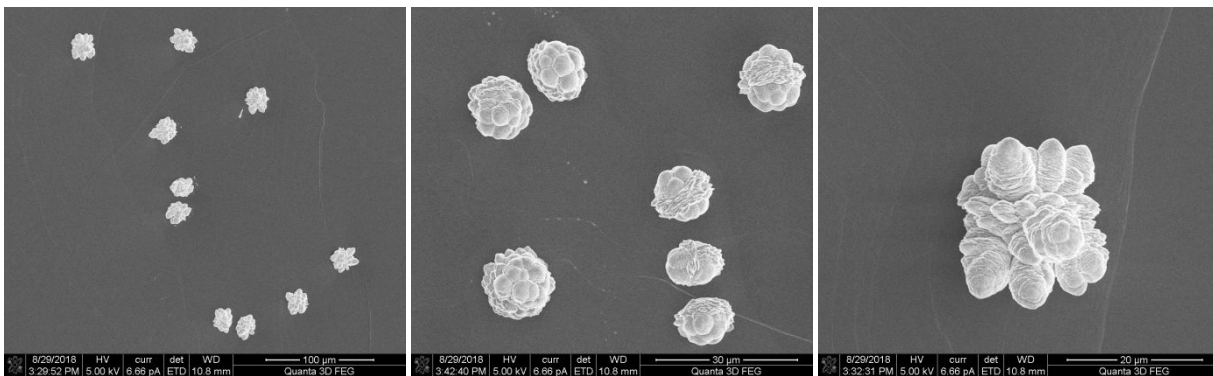

Figure S12: Images from the freshly cleaved HOPG surface after the experiment ended (σ = 5.85). Particle form is reminiscent of vaterite.

Dynamic force spectroscopy

Table S2: Binding parameters between the calcite {10.4} face and various SAMs.

SAM	f_{eq} (pN)	±*	x_t (pm)	±	k_{off} (s^{-1})	±	ΔG_b (kT)	±
COO(H)	124.0	3.9	97.5	21.0	14	13	5.0	0.68
NH$_2$	73.4	7.3	109.2	26.6	31	27	3.6	0.58
Mixed	48.4	4.1	98.2	48.2	125	125	2.3	0.76

* Uncertainty expressed as the standard deviation of the fit to Friddle model.[2]

Table S3: γ_{net} obtained from DFS measurements (Eq. 5) for different values of a for each of the three functionalized surfaces. h = 0.3.

Surface \ a (nm²)	0,2	0,3	0,4	0,5	0,6
COO(H)	103 ± 1	113 ± 1	118 ± 1	121 ± 1	124 ± 1
NH$_2$	111 ± 1	119 ± 1	123 ± 1	125 ± 1	126 ± 1
Mixed	120 ± 1	124 ± 1	127 ± 1	128 ± 1	129 ± 1

* Uncertainty propagated from the standard deviations for ΔG_b (Table S2).

Table S4: γ_{net} obtained from DFS measurements (Eq. 5) for different values of a for each of the three functionalized surfaces. h = 0.5.

Surface \ a (nm²)	0,2	0,3	0,4	0,5	0,6
COO(H)	103 ± 3	120 ± 2	129 ± 1	134 ± 1	137 ± 1
NH$_2$	117 ± 3	130 ± 2	136 ± 1	140 ± 1	142 ± 1
Mixed	131 ± 3	139 ± 2	143 ± 1	145 ± 1	147 ± 1

* Uncertainty propagated from the standard deviations for ΔG_b (Table S2).

COSMO-RS calculations

We calculated COSMO-RS interfacial free energies (γ) for alkane thiol dimers with various degrees of protonation. For the carboxylic SAMs, we obtained similar γ_{net} (101-102 mJ/m^2) for a fully protonated (*uncharged*) and half protonated surface (101-102 mJ/m^2). γ_{net} increases significantly for the fully deprotonated (*charged*) surface (136-159 mJ/m^2). γ_{net} of the primary amines was calculated for the uncharged (110-115 mJ m^{-2}) and single charged (+1) surface (108-112 mJ/m^2). For the 1:1 SAM, we calculated γ_{net} for a carboxyl-amine dimer sharing one proton (119-130 mJ/m^2).

Table S6: γ_{net} obtained using COSMO-RS calculations using h = 0.3 and h = 0.5.

Dimers	Charge	γ_{SL} (mJ/m^2) IP	γ_{CS} (mJ/m^2) calcite	γ_{net} (mJ/m^2) h = 0.3	γ_{net} (mJ/m^2) h = 0.5
COOH-COOH	0	-1	5,7	102	101
COO-H-COO	-1	4,3	6,6	102	101
COO-COO	-2	-174	-24,2	136	159
NH$_2$-NH$_2$	0	-29,8	-3	110	115
NH$_2$-H-NH$_2$	+1	-310	-101	108	112
COO-H-NH$_2$	0	-13,7	34,8	119	130

Resulting interfacial free energies

Table S8: γ_{net} determined from the three methods.

Surface	Nucleation studies (mJ/m^2)	DFS* (mJ/m^2)	COSMO-RS‡ (mJ/m^2) (charge)
Carboxyl SAM	77 (4)[!]	100-138	101-102, (0)
Amine SAM	100 (13)	110-143	110-115, (0)
Mixed SAM	n.a.	119-148	119-130 (0)
B28 peptoid	68 (11)	n.d.	n.d.

* the range represents γ_{net} values for different combinations of h and a (Table S3-S4), including the uncertainties.
‡ the range represents γ_{net} values for h=0.3 (lower value) and h=0.5 (higher value).
n.a.- not applicable, n.d.- not determined.
[!] errors propagated from the B parameter. The uncertainty for the amine SAM and B28 reflects few nucleation events.

REFERENCES:

(1) Parkhurst, D. L.; Appelo, C. A. J. User's Guide to PHREEQC (Version 2) : A Computer Program for Speciation, Batch-Reaction, One-Dimensional Transport, and Inverse Geochemical Calculations; Water-Resources Investigations Report; USGS Numbered Series 99–4259; U.S. Geological Survey : Earth Science Information Center, Open-File Reports Section [distributor], 1999.
(2) Friddle, R. W.; Noy, A.; Yoreo, J. J. D. Interpreting the Widespread Nonlinear Force Spectra of Intermolecular Bonds. Proc. Natl. Acad. Sci. **2012**, 109, 13573–13578. https://doi.org/10.1073/pnas.1202946109.